Published in final edited form as:
Mol Cell. 2006 September 01; 23(5): 697–707. doi:10.1016/j.molcel.2006.07.016.

Structure of an Hsp90 - Cdc37 - Cdk4 complex

Cara K. Vaughan[1], **Ulrich Göhlke**[2,§], **Frank Sobott**[3,†], **Valerie M. Good**[1], **Maruf M. U. Ali**[1], **Chrisostomos Prodromou**[1], **Carol V. Robinson**[3], **Helen R. Saibil**[2], and **Laurence H. Pearl**[1,*]

[1]Section of Structural Biology, The Institute of Cancer Research, Chester Beatty Laboratories, 237 Fulham Road, London SW3 6JB, UK

[2]Department of Crystallography, Birkbeck College, Malet Street, London WC1E 7HX, UK

[3]Cambridge University Chemical Laboratory, Lensfield Road, Cambridge, CB2 1EW, UK

Abstract

Activation of many protein kinases depends on their interaction with the Hsp90 molecular chaperone system. Recruitment of protein kinase clients to the Hsp90 chaperone system is mediated by the co-chaperone adaptor protein Cdc37, which acts as a scaffold, simultaneously binding protein kinases and Hsp90. We have now expressed and purified an Hsp90-Cdc37-Cdk4 complex, defined its stoichiometry, and determined its 3-dimensional structure by single-particle electron microscopy. Comparison with the crystal structure of Hsp90 allows us to identify the locations of Cdc37 and Cdk4 in the complex, and suggests a mechanism by which conformational changes in the kinase are coupled to the Hsp90 ATPase cycle.

Introduction

Association with the Hsp90 molecular chaperone system is an essential prerequisite for activation of an important set of protein kinases in the eukaryotic cell. The list of Hsp90s kinase ‘clientele’ includes key regulators such as PKB/Akt (Basso et al., 2002; Fontana et al., 2001; Sato et al., 2000), PDK1 (Fujita et al., 2002), LKB1 (Boudeau et al., 2003), Raf-1 (Grammatikakis et al., 1999; Schulte et al., 1995; Stancato et al., 1993), ErbB2 (Xu et al., 2001), Src-family kinases (Bijlmakers and Marsh, 2000; Xu and Lindquist, 1993; Xu et al., 1999), Aurora B (Lange et al., 2002), RIP (Lewis et al., 2000), components of the IκB kinase complex (Chen et al., 2002), and the cyclin-dependent kinases Cdk4, Cdk6 and Cdk9 (Mahony et al., 1998; Okeeffe et al., 2000; Stepanova et al., 1996). In all cases analysed, the Hsp90-dependent activation of the kinase is found to be dependent on the ATPase cycle of the chaperone (Prodromou et al., 2000) so that pharmacological inhibition by Hsp90-binding ATP-competitors (Prodromou et al., 1997; Roe et al., 1999; Stebbins et al., 1997) prevents client activation. As disregulation of many of these kinases is directly implicated in development and progression of cancer (Workman, 2004) understanding the molecular basis for kinase activation by Hsp90 is key to the development of new cancer chemotherapies.

*Correspondence to Prof. L.H. Pearl.
§Present Address: PSF biotech AG, Heubnerweg 6, 14059 Berlin, Germany.
†Present Address : Structural Genomics Consortium, University of Oxford, Botnar Research Centre, Oxford OX3 7LD, UK.

Europe PMC Funders Author Manuscripts

Recruitment of kinases to Hsp90 depends on Cdc37 (also known as $p50^{cdc37}$), originally discovered as a component of an Hsp90 complex with the viral oncogene v-Src (Brugge, 1986). Subsequently Cdc37 has been found associated with essentially all protein kinases whose activation is Hsp90-dependent (Pearl, 2005), including the cyclin dependent kinase Cdk4 (Dai et al., 1996; Fiore et al., 1997; Lamphere et al., 1997; Stepanova et al., 1996). Overexpression of Cdc37 is itself oncogenic, reflecting its association with many pro-oncogenic kinases, and suggesting that their Cdc37-dependent recruitment to the Hsp90 system may be limiting to their transforming potential (Stepanova et al., 2000a; Stepanova et al., 2000b). Cdc37 acts as a protein kinase-specific adaptor, recruiting client protein kinases to the Hsp90 system (Silverstein et al., 1998). Interaction of Cdc37 with protein kinases is mediated by the N-terminal segment (Grammatikakis et al., 1999; Shao et al., 2003a) while the middle and C-terminal regions of Cdc37 mediate interaction with Hsp90 (Roe et al., 2004; Shao et al., 2001; Zhang et al., 2004).

As with some other Hsp90 co-chaperones, Cdc37 regulates the conformationally-coupled ATPase mechanism of Hsp90, arresting the chaperone cycle in the client-loading phase, prior to Hsp90's ATP-dependent N-terminal dimerisation (Siligardi et al., 2002). The structural basis for this ability was revealed by a co-crystal structure of the N-terminal domain of Hsp90 in complex with the middle- and C-terminal segment of Cdc37 (Roe et al., 2004). Cdc37 binds to the 'lid' segment in the N-terminal domain of Hsp90, preventing its closure over the nucleotide binding site, and locking the N-terminal domains of the chaperone apart. This prevents the formation of the N-terminally dimerised 'tense' conformation of Hsp90 engendered by ATP binding (Chadli et al., 2000; Prodromou et al., 2000). Considerably less well understood is the basis of Cdc37's specific and selective binding to protein kinase clients. Minimally the intact N-terminal lobe of the kinase is required for interaction with Cdc37 (Prince and Matts, 2004; Scroggins et al., 2003) and the conserved glycine-rich loop plays a role in the interaction (Zhao et al., 2004). However this feature is present in many protein kinases that are not Hsp90 clients, and does not explain the high specificity of Cdc37. Similarly, the location of the interaction between the client kinase and Hsp90 itself in a Cdc37-scaffolded complex is also poorly described. Mutagenesis studies suggest involvement of residues in the middle segment of the chaperone (Basso et al., 2002; Fontana et al., 2002; Meyer et al., 2003; Sato et al., 2000) but the nature of the interaction and how Hsp90 association activates the bound kinase remains obscure.

Key to understanding the Hsp90/Cdc37-dependent activation of protein kinase clients is the ability to study the structure and biochemistry of defined complexes *in vitro*. We have developed a recombinant system that allows production of assembled ternary Hsp90 – Cdc37 – kinase complexes at a milligram level. Using this we have purified an Hsp90-Cdc37-Cdk4 complex to homogeneity, defined its stoichiometry, and determined its three-dimensional structure by single-particle reconstruction from negative-stain electron microscopy. Comparison with the crystal structure of an Hsp90 dimer in the ATP-bound conformation (Ali et al., 2006) allows the identification of the chaperone domains and the location of Cdc37 and Cdk4 in the complex, providing the first structural view of client protein bound to the Hsp90 molecular chaperone, and suggesting a mechanism for coupling the Hsp90 ATPase cycle to conformational changes in bound client protein kinases.

Results

Isolation and compositional analysis of Hsp90 - Cdc37 - protein kinase complex

Recombinant expression of Hsp90, Cdc37 and several protein kinase clients in isolation, has been reported previously by ourselves and others. However, assembly of well-behaved and stoichiometric Hsp90-Cdc37-kinase complexes by mixing purified proteins *in vitro* has proved refractory, suggesting that other cellular factors are probably involved in the client loading process. We sought to bypass this problem by co-expressing components using a baculovirus vector in *Sf9* cells (see Methods). Using this system we could express His_6-tagged human Cdk4 and human B-Raf catalytic domain at useful levels, in the presence of co-expressed human Cdc37. Fractionation of cell lysates using immobilised metal affinity chromatography (IMAC), yielded co-eluting Cdk4 and Cdc37, as well as an ~83 kDa protein. This was subsequently identified by mass spectrometry as the *Spodoptera frugiperda* Hsp90 homologue, which is > 70% sequence identical to human Hsp90α. Subsequent purification yielded distinct fractions containing **H**sp90, **C**dc37 and Cd**k**4 (H-C-K) (Figure 1a) or **C**dc37 and Cd**k**4 (C-K) (Figure 2a) which eluted as single peaks in an analytical gel-filtration column indicating that they are homogenous ternary and binary complexes respectively (Figure 1c, 2b).

Previous studies have shown that in the absence of a client kinase, Cdc37 and Hsp90 interact *in vitro* as dimers to form a $(Cdc37)_2 – (Hsp90)_2$ complex (Roe et al., 2004; Roiniotis et al., 2005; Zhang et al., 2004). To determine the stoichiometries of the *in vivo* assembled H-C-K and C-K complexes they were injected using nano-electrospray ionisation into a modified tandem time-of-flight mass-spectrometer (Waters Q-Tof2), that allows analysis of assembled protein complexes by minimising the energy of molecular collisions and consequent dissociation of components (Sobott et al., 2002). M/z spectra for the H-C-K complex identified the presence of an $(Hsp90)_2$-Cdc37-Cdk4 complex in addition to some uncomplexed protein generated by collisions in the spectrometer, but no larger species (Figure 1d, e). This stoichiometry is consistent with densitometry of the Coomassie stained complex, which showed a 1:1 ratio of Cdc37 to Cdk4. The unusually heavy staining of Hsp90 is also consistent with our densitometry, which revealed Hsp90 to bind Coomassie in a non-linear fashion when calibrated against Cdc37 and Cdk4 (Figure 1b). M/z spectra for the C-K fraction showed the presence of a $(Cdc37)_2$-Cdk4 complex in addition to some uncomplexed protein generated by collisions in the spectrometer, but no larger assemblies (Figure 2c, d). As the 2:1:1 stoichiometry of the H-C-K complex was unexpected, and in contradiction of our previous predictions (Roe et al., 2004), we sought to determine whether this was unique to complexes with Cdk4, or whether it represents the normal stoichiometry for stable Hsp90-Cdc37-kinase complexes. We therefore co-expressed the His_6-tagged kinase domain of B-Raf with Cdc37 in *Sf9* cells (Wan et al., 2004) and purified a B-Raf H-C-K complex in a similar fashion. As with the Cdk4 complex, modified QTOF mass spectrometry of the B-Raf H-C-K complex identified an $(Hsp90)_2$-Cdc37-B-Raf complex as the largest species (Suppl. Figure 1).

Electron microscopy and 3D reconstruction of an $(Hsp90)_2$–Cdc37–Cdk4 complex

The small asymmetric H-C-K complex particles (~245 kDa) were visualised in the electron microscope at 42000 x magnification, stained with 2% uranyl acetate (Figure 3a). 4231 individual particles were picked and aligned, and grouped into classes using multivariate statistical analysis and hierarchical ascendant classification (see Methods). Stable representative classes were used to generate a 3D volume by angular reconstitution, which was iteratively refined to give the final model. Reprojections of the final model correspond well to the raw data (Figure 3b) and to the original classes from before the angular reconstitution, unbiased by the refinement process (Suppl. Figure 2a). Particles showed a good angular distribution with no significant problems of preferred orientation (Suppl. Figure 2b). The resolution of the structure estimated from the Fourier Shell Correlation coefficient of 0.5, is ~19Å (Suppl. Figure 2c).

The reconstructed H-C-K complex has an elongated structure, ~140-150 Å long and ~85-95 Å diameter, resembling a candle-flame; pointed at one end and rounded at the other (Figure 4a). Two columns of density twist around the long axis, connecting the base to the narrower tip (Figure 4b). A stain-filled cavity evident in class sums corresponds to a channel of oval cross-section running through the 3D structure, perpendicular to the long axis. Views from opposite sides have many similarities, and there is an overall rough 2-fold symmetry to the structure around the long axis. However consistent with the 2:1:1 composition of the complex, this symmetry is approximate and is clearly broken by asymmetric distribution of density at the base and by a tilt to one side of the tip of the candle flame.

Fitting of Protein Chains

Comparison of the 3D reconstruction with the crystal structure of an Hsp90 dimer (Ali et al., 2006), shows many points of similarity, validating our angular reconstitution for this asymmetric complex (Figure 4c). Both crystal and EM structures have very similar overall shapes and dimensions, with a pointed and a rounded end; both structures have a narrow channel running through them; and both structures twist around the long axis (Figure 5a,b). The handedness of this latter feature allows the hand of the EM reconstruction to be fixed (Figure 5c). It is immediately evident from comparison with the crystal structure that the narrow tip of the EM volume corresponds to the constitutively dimerised C-terminal domains of Hsp90. The two partially symmetric longitudinal columns of density therefore correspond to the two Hsp90 monomers, with the N-terminal domains contributing to the rounded base of the reconstruction.

The columns of density connecting the tip and base are very similar in overall shape to monomers of Hsp90 from the crystal structure, and features corresponding to the three main segments of the Hsp90 crystal structure are readily discernable (Figure 5a, b). The individual monomers from the dimeric Hsp90 crystal structure could be readily docked into the density manually, maintaining the C-terminal dimerisation interface. Small changes in domain orientation, achieved by hinging at the loop regions linking the domains, allow an excellent fit of the monomers to the reconstruction (Figure 6a). These segments of polypeptide are known to display considerable flexibility (see Discussion).

The N-terminal dimerisation found in the crystal structure is not seen in the complex. Instead the N-terminal domain of one monomer is hinged backwards, away from its counterpart in the other monomer, such that its relative orientation with respect to the middle domain is opened like a jaw. For the second monomer the largest change in domain orientation is between the C-terminal and middle domains, whereas orientation of the N-terminal domain relative to the middle domain is similar to that found in the crystal structure.

As well as the two Hsp90 molecules, the density of the EM reconstruction must account for the single Cdc37 and Cdk4 molecules present in the complex. The globular domain in the C-terminal half of Cdc37 has previously been shown to interact with the N-domain of Hsp90, binding to the ‘lid’ and open mouth of the nucleotide-binding pocket, and preventing its interaction with the middle segment of the chaperone (Roe et al., 2004). The Hsp90 N-terminal domain from the crystal structure of the Hsp90-Cdc37 complex can be superposed onto the N-terminal domain of the ‘open’ Hsp90 monomer (Figure 6a) in the EM reconstruction. This positions the Cdc37 C-terminal globular domain neatly into unoccupied density between the densities assigned to the two N-terminal domains of Hsp90.

The remaining unoccupied globular density is a bilobal segment bridging the base of the structure to half way up one of the longitudinal columns. The lobes are of unequal size; the lower lobe, associated with the base of the reconstruction, is smaller than the upper lobe contacting the middle of one longitudinal column. The sizes of these lobes are consistent with the N-terminal and C-terminal lobes respectively of a cyclin-dependent kinase catalytic domain (Figure 6a).

There is no distinct globular density that can be assigned to the N-terminal segment of Cdc37, whose structure is currently unknown. However, there is continuous extra density around the N-terminal domain of the second Hsp90 (Figure 6b). The orientation of the docked C-terminal Cdc37 globular domain directs the helix connecting to the N-terminal domain into this extra density. As we find that Cdc37-pSer13 in the complex is highly resistant to dephosphorylation (data not shown) the N-terminus of Cdc37 appears to be considerably buried in the complex, and it is likely that it is subsumed in the density at the base of the reconstruction, closely associated with the Hsp90 N-terminal domains and the kinase, and probably in contact with both. No density for the C-terminal tail of Cdc37 is visible in the reconstruction, however on the basis of the orientation of the docked Cdc37 globular domain, this helical segment would be directed out of the complex into solvent and unlikely to be well ordered. Indeed in the crystal structure of Cdc37 bound to the N-terminus of Hsp90 the C-terminal tail displayed high temperature factors and was only visible as a result of a fortuitous crystal contact (Roe et al., 2004). Consistent with the lack of any direct involvement of this C-terminal tail in the complex, the corresponding region has been shown to be substantially dispensable for full biological function in yeast (Lee et al., 2002).

Discussion

Conformation Flexibility of Hsp90

Comparison of Hsp90 crystal structures illustrates the molecule's considerable flexibility. For example, alignment of the middle domains of yeast Hsp90 (Ali et al., 2006) with their equivalent in the *E. coli* homologue HtpG (Huai et al., 2005), reveals a huge translation and rotation of the N-domain in each structure with respect to the other, such that the β-sheets therein are now at right angles. This degree of flexibility within the confines of a crystal lattice reflect a much greater conformational variability revealed by analysis of the Hsp90 dimer in solution (Zhang et al., 2004). Indeed difficulty in obtaining highly diffracting crystals of the full-length protein can be attributed to this conformational variability. Success was ultimately dependent on trapping Hsp90 in a defined functional and conformational state, in complex with nucleotide and the co-chaperone p23/Sba1 (Ali et al., 2006).

Biochemical and structural data to date support an ATP-driven molecular clamp mechanism (Prodromou et al., 2000; Siligardi et al., 2004), and large conformational changes of the type described above are a prerequisite for this. The Hsp90 dimer, constitutively dimerised via its C-terminal domains, cycles between a state in which the N-terminal domains are in an open ATP-free conformation, either held apart in a rigid manner by a dimer of the co-chaperone Cdc37 (Roe et al., 2004) or simply unconstrained, and a closed or tense state in which ATP is bound and a lid closed over the ATP-binding site to expose a second, transient dimerisation interface between the two N-terminal domains (Ali et al., 2006; Prodromou et al., 2000).

The flexibility required for such large structural changes can been attributed to two linker regions that join the N- to middle, and middle to C-terminal domains. The flexibility of these linkers is evident from their susceptibility to proteolysis, and the stability of the domains they connect when expressed in isolation. In our model, the crystal structure of full-length Hsp90 fits into the EM reconstruction with relatively small adjustments of these linker regions. The dynamic nature of Hsp90's structure is therefore important not only for the hydrolysis of ATP (Prodromou et al., 2000) and co-chaperone binding (Meyer et al., 2004; Roe et al., 2004) but also for enabling Hsp90 to adopt conformations, such as we see in the current reconstruction, which allow client protein binding.

Protein Kinase and Cdc37 Interactions

A significant number of protein kinases form complexes with Hsp90 and Cdc37 as a prerequisite to their activation (reviewed in (Pearl, 2005)) but the stoichiometry of these complexes has not previously been determined. For Cdk4 and for B-Raf we have now observed a stable complex containing an Hsp90 dimer bound to single molecules of Cdc37 and the kinase, affinity purified via the tagged kinase. Whether this stoichiometry is common to all kinase clients of Hsp90 is not known, but that it occurs with two such distantly related kinases suggests that this is likely to be the case. By contrast, the Cdc37-Cdk4 complex devoid of Hsp90, contains a single kinase bound to a dimer of Cdc37. We and others have previously shown formation of an Hsp90-Cdc37 complex in the absence of any kinase, consisting of dimers of each (Roe et al., 2004; Roiniotis et al., 2005; Zhang et al.,

2004). Cdc37 is a dimer in isolation, but its dissociation constant is low micromolar (Siligardi et al., 2002), suggesting that it can exist happily in dimer or monomer form. Taken together these data point to an ordered process of kinase client loading in which a kinase-$(Cdc37)_2$ complex initially binds to an Hsp90 dimer via a symmmetrical $(Cdc37)_2$-$(Hsp90)_2$ dimer-dimer interaction as previously suggested (Roe et al., 2004), that simultaneously arrests the ATPase cycle of Hsp90 (Siligardi et al., 2002). Subsequent conformational rearrangement of that initial complex could then release a Cdc37 molecule to give the stable asymmetrical $(Hsp90)_2$-Cdc37-kinase complexes reported here (Suppl. Figure 3). While this idea is fully consistent with the data, further work will be required to substantiate it.

The channel between the Hsp90 protomers in the complex, clearly contradicts previous models (Roe et al., 2004) in which a client is bound between the two Hsp90 molecules in an analogy to ‘barrel’ chaperonins such as GroEL or CCT (Saibil, 2000). Instead, the client is bound to the outer edge of one Hsp90 molecule, bridging its N- and middle segments. The density attributed to Cdk4 is distinctly bilobal, suggesting that the two lobes of the kinase are in an extended conformation compared with the mature protein. This could have consequences for the ability of the kinase to bind nucleotide, since motifs from both lobes contribute to the ATP-binding site. Whether Cdk4 is competent to bind ATP, cyclins or CDK inhibitory proteins when part of the Hsp90-Cdc37 complex is now the focus of further work in our laboratory.

The larger lobe of the kinase clearly interacts with the middle segment of one Hsp90 monomer, while the other lobe is in a position to interact with the associated Hsp90 N-terminal domain and/or N-terminal part of the Cdc37 molecule anchored on the other Hsp90 N-terminal domain; these possibilities cannot be distinguished in the present structure and may occur simultaneously. This complex mode of interaction is consistent with studies analysing sites of interaction between Hsp90, Cdc37, and a range of client protein kinases including ErbB2 (Xu et al., 2005), HRI (Scroggins et al., 2003), Lck (Prince and Matts, 2004), as well as Cdk4 (Zhao et al., 2004) that implicate the N-terminal lobe of the kinase as essential for interactions with Hsp90 and Cdc37, while regions in the kinase C-terminus are involved in Hsp90 binding only. Our interpretation of the bilobal segments based on their size (see Results) is fully consistent with these analyses. In addition, the larger lobe of the kinase density comes close to a hydrophobic patch centred on Trp 300 in the middle segment of Hsp90, and shown by mutagenesis to be involved in client protein binding (Meyer et al., 2003) (Figure 7). Part of this patch is contributed by residues 328-338, which form an amphipathic loop projecting from the body of the middle segment. The considerable flexibility of this loop would give a degree of tolerance allowing interaction with a range of client proteins.

The bivalent interaction of the Cdk4, with one lobe binding to the middle segment of Hsp90 and the other to the N-terminal domain and/or Cdc37, provides a clear mechanism for coupling ATP-dependent changes in the relative conformation of the N- and middle segments of Hsp90 (Chadli et al., 2000; Prodromou et al., 2000), to changes in the orientation of the N- and C-lobes of the bound kinase. As the relative positioning of these lobes and the segment of protein that links them is well known to play a significant role in regulating activity of many protein kinases (Johnson et al., 1996), association with Hsp90

might be required to facilitate the switch from an inactive to an active conformation in those kinases where there is a high activation barrier to that conformational change.

The N-terminal domain of Cdc37 has consistently been shown to be necessary for kinase binding (Grammatikakis et al., 1999; Shao et al., 2001), while its C-terminus is responsible for interaction with Hsp90 (Roe et al., 2004; Shao et al., 2001; Zhang et al., 2004). Nonetheless, the extreme N-terminal part of Cdc37 also plays a role in Hsp90 interactions in the context of a client protein complex. Thus, while mutation of residues 2-4 of Cdc37 compromise binding of a client kinase but do not affect Hsp90 binding (Scroggins et al., 2003), mutation of Trp 7 results in both reduced client and Hsp90 binding. Phosphorylation of Ser 13 in Cdc37 has been shown to be essential for formation of productive Hsp90-Cdc37-client complexes, but mutation of this residue has no apparent effect on direct Hsp90-Cdc37 interaction (Miyata and Nishida, 2004; Shao et al., 2003b). We find this phosphorylation to be present in the purified baculovirus-expressed Cdc37, and in $(Hsp90)_2$-Cdc37-Cdk4 complexes. pSer 13 in free Cdc37 is rapidly dephosphorylated by phosphatase treatment, however in marked contrast, pSer 13 in the ternary $(Hsp90)_2$-Cdc37-Cdk4 complex was resistant to dephosphorylation, consistent with its burial in the complex (data not shown). Taken together, these data suggest that the extreme N-terminal segment of Cdc37 incorporating pSer 13 cements the interaction between Hsp90 and the kinase client, possibly becoming bound between them in the ternary complex.

In our model, the N-terminal segment of Cdc37 would stretch across the base of the complex towards the bound Cdk4 and the other Hsp90 N-terminal domain, allowing residues at its N-terminus to interact with both as suggested by the mutational and accessibility data. This is also consistent with the additional observation that the residues in Cdc37 that connect its N-terminal and C-terminal domains regulate both Hsp90 and kinase binding, since it is this sub-domain of Cdc37 which would bridge between the N-terminal domains of the two Hsp90 monomers (Shao et al., 2003b).

A recent study examining the client-binding site on Cdc37 isolated a hydrophobic 20-residue peptide corresponding to residues 181-200 of Cdc37 that could apparently co-precipitate Raf-1 kinase domain from Cos-7 cells (Terasawa and Minami, 2005). The significance of this observation is uncertain, as these residues are substantially buried in the globular domain of Cdc37 that binds the N-terminal domain of Hsp90 (Roe et al., 2004). Furthermore these results directly conflict with earlier studies in Cos-1 and Sf9 cells which showed the Raf-1 kinase binding site on Cdc37 resides in the N-terminal half of the protein (residues 1-164) (Grammatikakis et al., 1999), and that truncation of Cdc37 beyond residue 164 results in loss of Hsp90 from the Cdc37-Raf-1 complex, consistent with our crystallographic data (Roe et al., 2004).

Conclusion

The EM reconstruction presented here provides a first experimental view of a client-loaded Hsp90 complex, consistent with a large body of crystallographic, biochemical and genetic data. This complex was isolated in the presence of sodium molybdate, which has been widely used to stabilise complexes of steroid hormone receptors and other transcription factors with Hsp90 (Pratt and Toft, 1997), and has the same effect here (see Methods).

Molybdate is believed to act as a mimetic of the ATP γ-phosphate, occupying Hsp90's ATP binding site in combination with ADP to inhibit the ATPase cycle and trap the complex with the client in a pre-activated 'early' state. The precise position in the chaperone cycle that our reconstruction represents is not known. However the presence of one Cdc37 molecule suggests that it is also an early complex, trapped somewhere between initial complex formation, which involves a Cdc37 dimer (Siligardi et al., 2002; Zhang et al., 2004), and the catalytically-competent ATP-bound conformation (Ali et al., 2006), progression to which requires complete disengagement of Cdc37 from the Hsp90 N-domains. In any event, this complex is only one of a number of modes of interaction that a client makes with Hsp90 and Cdc37 during the chaperone's ATPase cycle, and further work will be required to identify and isolate the other client-bound intermediates that may occur. While the present work defines the composition and architecture of the Hsp90-Cdc37-kinase complex for the first time, many key questions relating to the detailed interactions involved, remain to be answered. It is only those details that will lead to a full understanding of how Hsp90 and Cdc37 facilitate activation of client protein kinases, and what features of the client proteins are responsible for their specific requirement for, and recruitment to, the Hsp90-Cdc37 chaperone system. Full activation of Cdk4, downstream of Hsp90-binding, requires phosphorylation of the activation loop, and complexation with Cyclin D (Kato et al., 1994). Whether these steps take place in the context of Hsp90 is at present unknown, but the Hsp90-Cdc37-Cdk4 complex provides a robust system with which to address these questions.

Methods

Expression and Purification of Proteins

A modified pFastbac DUAL (Invitrogen) expression vector was made by inserting an intergenic region, encoding a 6-His tag, between BamHI and EcoRI of Multiple Cloning Site I (MCS I). This modification also encoded an NheI restriction site immediately 3' to the 6-His tag. Cdk4 was amplified by PCR encoding both a BamHI and NheI restriction site and a PreScission cleavage site 5' to the gene, and a 3' HindIII restriction site. The BamHI-HindIII fragment was cloned into pET28a (Novagen). Subsequently the NheI-NotI fragment was cloned into our modified MCS I of pFastbac DUAL. Cloning of Cdc37 has been described previously (Siligardi et al., 2002). A XhoI/KpnI PCR fragment of Cdc37 was cloned into MCS II of the pFastbac DUAL vector.

Proteins were expressed in *Sf9* cells over three days. The cell pellet was lysed by homogenisation in TBS-Mo buffer [25 mM Tris.HCl pH 7.5, 150 mM NaCl, 10 mM KCl, 10 mM $MgCl_2$, 20 mM Na_2MoO_4] with 25 mM NaF, 25 mM β-sodium glycerophosphate and EDTA-free Complete protease inhibitor tablets (Roche). Cdc37 and Cdk4 co-eluted with endogenous *Sf9* Hsp90 (H-C-K) from Talon resin (BD Bioscience). Gel filtration on a Superdex200 HR column (GE Healthcare) with TBS-Mo buffer, desalting into TBS-Mo without NaCl, followed by ion-exchange using Q-Source resin (GE Healthcare), and analytical gel filtration on a Superose 6 HR10/30 (GE Healthcare) column with TBS-Mo buffer were used to purify the complex to homogeneity. The complex could also be isolated using the same protocol in the absence of sodium molybdate, however the yields were

considerably reduced. Baculovirus expressed Hsp90-Cdc37-B-Raf complex was purifed as described (Wan et al., 2004).

Nano-ESI TOF-MS

Samples for MS analysis were buffer exchanged into 100 mM ammonium acetate pH 7 using Micro Bio-Spin 6 columns (Bio-Rad). Nano-ESI capillaries were prepared in-house from borosilicate glass tubes of 1 mm outer and 0.5 mm inner diameter (Harvard Apparatus, Holliston, MA) using a Flaming/Brown P-97 micropipette puller (Sutter Instruments, Hercules, CA) and gold-coated using a sputter coater (Quorum Technologies, Newhaven, United Kingdom). Capillary tips were cut under a stereo-microscope to give inner diameters of 1–5 μm, and typically 2 μL of solution were loaded for sampling. Mass spectra were recorded on a tandem-mass spectrometer (Waters Q-Tof2, Manchester, UK) which was modified for high mass operation (Sobott et al., 2002), and pressures and accelerating potentials were adjusted to preserve noncovalent interactions (Heck and Van Den Heuvel, 2004; Sobott and Robinson, 2002). Data were acquired and processed with MassLynx software (Waters, Manchester, UK).

Electron Microscopy

HCK complex at 10-15 μg/ml was stained on carbon-coated copper grids with 2% (w/v) uranyl acetate after glow discharging in the presence of pentyl-amine. Samples were imaged in a FEI Tecnai T12 electron microscope (FEI, Eindhoven, NL) operating at 120 kV, and recorded in low dose mode at a defocus of around 0.5 μm on Kodak SO163 film at 42000 x magnification. Micrographs were digitised on a Zeiss Photoscan LD linear array scanner at 14 μ/pixel (3.33 Å/pixel at the specimen level).

Image Processing

Defocus and astigmatism were determined using CTFfind3 (Mindell and Grigorieff, 2003). Boxed particles from 35 micrographs were imported into IMAGIC (van Heel et al., 1996) for all further processing. 4231 particles were centred using 3 rounds of translational alignment to the rotationally averaged total sum. Multivariate statistical analysis and hierarchical ascendant classification was used to generate reference classes to which all particles were aligned. This process was repeated iteratively. Well-defined classes representing distinct views of the complex were for chosen for angular reconstitution to generate an initial model. Additional classes were incorporated into the model with increasing Euler angle precision in 3 rounds of anchor set refinement.

At this point the reconstruction was 3D-masked and refined by projection matching. For each iteraction the angle assignments were sorted by reprojection error (agreement between the average for each orientation and the corresponding reprojection) and visually checked to ensure that the classes were acceptable. A 3D map was then created from the acceptable classes.

The model was determined to be fully refined after 8 rounds of projection matching when the percentage of total particles changing class between successive rounds and the value of the Fourier Shell Correlation (FSC) coefficient at 0.5 had converged. At this stage there was

Europe PMC Funders Author Manuscripts

no visible change in the reconstruction between rounds of refinement. The final reconstruction was generated using 190 out of a total of 412 class sums, containing 76.8% of the data, but a map with all 412 sums was not noticeably different.

Model Building

The anti-clockwise twist of the crystal structure of full length Hsp90 (Ali et al., 2006) was used to assign the hand of the EM map.

All crystal structures used for model building (Hsp90 PDB code 2CGE,2CG9, Cdk6 PDB code 1J0W, N-Hsp90 – C-Cdc37 PDB code 1US7) were filtered to 20 Å using the Situs program PDBlur (Wriggers et al., 1999) to allow a direct comparison with the EM reconstruction. All docking was carried out manually in MacPyMOL (www.pymol.org).

Supplementary Material

Refer to Web version on PubMed Central for supplementary material.

Acknowledgments

We are very grateful to Paul Wan and Chris Marshall for the kind gifts of B-Raf–Hsp90-Cdc37 complex and Cdk4 cDNA respectively, to Vivienne Thompson and Sara Kisakye-Nambozo for assistance with baculovirus expression and Elena Orlova for help with angular reconstitution. This work was supported by BBSRC (HS) and the Wellcome Trust (LHP)

References

Ali MM, Roe SM, Vaughan CK, Meyer P, Panaretou B, Piper PW, Prodromou C, Pearl LH. Crystal structure of an Hsp90-nucleotide-p23/Sba1 closed chaperone complex. Nature. 2006; 440:1013–1017. [PubMed: 16625188]

Basso AD, Solit DB, Chiosis G, Giri B, Tsichlis P, Rosen N. Akt forms an intracellular complex with heat shock protein 90 (Hsp90) and Cdc37 and is destabilized by inhibitors of Hsp90 function. J Biol Chem. 2002; 277:39858–39866. [PubMed: 12176997]

Bijlmakers MJ, Marsh M. Hsp90 is essential for the synthesis and subsequent membrane association, but not the maintenance, of the Src-kinase p56(lck). Mol Biol Cell. 2000; 11:1585–1595. [PubMed: 10793137]

Boudeau J, Deak M, Lawlor MA, Morrice NA, Alessi DR. Heat-shock protein 90 and Cdc37 interact with LKB1 and regulate its stability. Biochem J. 2003; 370:849–857. [PubMed: 12489981]

Brugge JS. Interaction of the Rous sarcoma virus protein pp60v-src withthe cellular proteins pp50 and pp90. Curr Top Microbiol Immunol. 1986; 123:1–22. [PubMed: 2419040]

Chadli A, Bouhouche I, Sullivan W, Stensgard B, McMahon N, Catelli MG, Toft DO. Dimerization and N-terminal domain proximity underlie the function of the molecular chaperone heat shock protein 90. Proc Natl Acad Sci USA. 2000; 97:12524–12529. [PubMed: 11050175]

Chen G, Cao P, Goeddel DV. TNF-induced recruitment and activation of the IKK complex require Cdc37 and Hsp90. Mol Cell. 2002; 9:401–410. [PubMed: 11864612]

Dai K, Kobayashi R, Beach D. Physical interaction of mammalian CDC37 with CDK4. J Biol Chem. 1996; 271:22030–22034. [PubMed: 8703009]

Fiore F, Lamphere L, Xu X, Brizuela L, Keezer S, Sardet C, Draetta GF, Gyuris J. Interaction between CDC37 and Cdk4 in human cells. European Journal of Cell Biology. 1997; 72:74.

Fontana J, Fulton D, Chen Y, Fairchild TA, McCabe TJ, Fujita N, Tsuruo T, Sessa WC. Domain mapping studies reveal that the M domain of hsp90 serves as a molecular scaffold to regulate Akt-dependent phosphorylation of endothelial nitric oxide synthase and NO release. CircRes. 2002; 90:866–873.

Fontana JT, Fulton D, McCabe TJ, Sessa WC. Hsp90 serves as a scaffold for Akt induced eNOS phosphorylation. Circulation. 2001; 104:507.

Fujita N, Sato S, Ishida A, Tsuruo T. Involvement of Hsp90 in signaling and stability of 3-phosphoinositide-dependent kinase-1. J Biol Chem. 2002; 277:10346–10353. [PubMed: 11779851]

Grammatikakis N, Lin J-H, Grammatikakis A, Tsichlis PN, Cochran BH. p50cdc37 acting in concert with Hsp90 is required for Raf-1 function. Mol Cell Biol. 1999; 19:1661–1672. [PubMed: 10022854]

Heck AJ, Van Den Heuvel RH. Investigation of intact protein complexes by mass spectrometry. Mass Spectrom Rev. 2004; 23:368–389. [PubMed: 15264235]

Huai Q, Wang H, Liu Y, Kim HY, Toft D, Ke H. Structures of the N-terminal and middle domains of E. coli Hsp90 and conformation changes upon ADP binding. Structure (Camb). 2005; 13:579–590. [PubMed: 15837196]

Johnson LN, Noble MEM, Owen DJ. Active and inactive protein kinases: Structural basis for regulation. Cell. 1996; 85:149–158. [PubMed: 8612268]

Kato JY, Matsuoka M, Strom DK, Sherr CJ. Regulation of cyclin D-dependent kinase 4 (cdk4) by cdk4-activating kinase. Mol Cell Biol. 1994; 14:2713–2721. [PubMed: 8139570]

Lamphere L, Fiore F, Xu X, Brizuela L, Keezer S, Sardet C, Draetta GF, Gyuris J. Interaction between Cdc37 and Cdk4 in human cells. Oncogene. 1997; 14:1999–2004. [PubMed: 9150368]

Lange BM, Rebollo E, Herold A, Gonzalez C. Cdc37 is essential for chromosome segregation and cytokinesis in higher eukaryotes. EMBO J. 2002; 21:5364–5374. [PubMed: 12374737]

Lee P, Rao J, Fliss A, Yang E, Garrett S, Caplan AJ. The Cdc37 protein kinase-binding domain is sufficient for protein kinase activity and cell viability. J Cell Biol. 2002; 159:1051–1059. [PubMed: 12499358]

Lewis J, Devin A, Miller A, Lin Y, Rodriguez Y, Neckers L, Liu ZG. Disruption of hsp90 function results in degradation of the death domain kinase, receptor-interacting protein (RIP), and blockage of tumor necrosis factor-induced nuclear factor-kappaB activation. J Biol Chem. 2000; 275:10519–10526. [PubMed: 10744744]

Mahony D, Parry DA, Lees E. Active cdk6 complexes are predominantly nuclear and represent only a minority of the cdk6 in T cells. Oncogene. 1998; 16:603–611. [PubMed: 9482106]

Meyer P, Prodromou C, Hu B, Vaughan C, Roe SM, Panaretou B, Piper PW, Pearl LH. Structural and functional analysis of the middle segment of Hsp90: Implications for ATP hydrolysis and client-protein and co-chaperone interactions. Mol Cell. 2003; 11:647–658. [PubMed: 12667448]

Meyer P, Prodromou C, Liao C, Hu B, Mark Roe S, Vaughan CK, Vlasic I, Panaretou B, Piper PW, Pearl LH. Structural basis for recruitment of the ATPase activator Aha1 to the Hsp90 chaperone machinery. EMBO J. 2004; 23:511–519. [PubMed: 14739935]

Mindell JA, Grigorieff N. Accurate determination of local defocus and specimen tilt in electron microscopy. J Struct Biol. 2003; 142:334–347. [PubMed: 12781660]

Miyata Y, Nishida E. CK2 controls multiple protein kinases by phosphorylating a kinase-targeting molecular chaperone, Cdc37. Mol Cell Biol. 2004; 24:4065–4074. [PubMed: 15082798]

Okeeffe B, Fong Y, Chen D, Zhou S, Zhou Q. Requirement for a kinase-specific chaperone pathway in the production of a Cdk9/cyclin T1 heterodimer responsible for P-TEFb-mediated tat stimulation of HIV-1 transcription. J Biol Chem. 2000; 275:279–287. [PubMed: 10617616]

Pearl LH. Hsp90 and Cdc37 -- a chaperone cancer conspiracy. Curr Opin Genet Dev. 2005; 15:55–61. [PubMed: 15661534]

Pratt WB, Toft DO. Steroid receptor interactions with heat shock protein and immunophilin chaperones. Endocr Rev. 1997; 18:306–360. [PubMed: 9183567]

Prince T, Matts RL. Definition of protein kinase sequence motifs that trigger high affinity binding of Hsp90 and Cdc37. J Biol Chem. 2004; 279:39975–39981. [PubMed: 15258137]

Prodromou C, Panaretou B, Chohan S, Siligardi G, O'Brien R, Ladbury JE, Roe SM, Piper PW, Pearl LH. The ATPase cycle of Hsp90 drives a molecular 'clamp' via transient dimerization of the N-terminal domains. EMBO J. 2000; 19:4383–4392. [PubMed: 10944121]

Prodromou C, Roe SM, O'Brien R, Ladbury JE, Piper PW, Pearl LH. Identification and structural characterization of the ATP/ADP-binding site in the Hsp90 molecular chaperone. Cell. 1997; 90:65–75. [PubMed: 9230303]

Roe SM, Ali MM, Meyer P, Vaughan CK, Panaretou B, Piper PW, Prodromou C, Pearl LH. The Mechanism of Hsp90 regulation by the protein kinase-specific cochaperone p50(cdc37). Cell. 2004; 116:87–98. [PubMed: 14718169]

Roe SM, Prodromou C, O.Brien R, Ladbury JE, Piper PW, Pearl LH. The Structural Basis for Inhibition of the Hsp90 Molecular Chaperone, by the Anti-tumour Antibiotics Radicicol and Geldanamycin. J Med Chem. 1999; 42:260–266. [PubMed: 9925731]

Roiniotis J, Masendycz P, Ho S, Scholz GM. Domain-mediated dimerization of the Hsp90 cochaperones Harc and Cdc37. Biochemistry. 2005; 44:6662–6669. [PubMed: 15850399]

Saibil H. Molecular chaperones: containers and surfaces for folding, stabilising or unfolding proteins. Curr Opin Struct Biol. 2000; 10:251–258. [PubMed: 10753820]

Sato S, Fujita N, Tsuruo T. Modulation of akt kinase activity by binding to hsp90. Proc Natl Acad Sci U S A. 2000; 97:10832–10837. [PubMed: 10995457]

Schulte TW, Blagosklonny MV, Ingui C, Neckers L. Disruption of the Raf-1-Hsp90 molecular complex results in destabilization of Raf-1 and loss of Raf-1-Ras association. J Biol Chem. 1995; 270:24585–24588. [PubMed: 7592678]

Scroggins BT, Prince T, Shao J, Uma S, Huang W, Guo Y, Yun BG, Hedman K, Matts RL, Hartson SD. High affinity binding of Hsp90 is triggered by multiple discrete segments of its kinase clients. Biochemistry. 2003; 42:12550–12561. [PubMed: 14580201]

Shao J, Grammatikakis N, Scroggins BT, Uma S, Huang WJ, Chen JJ, Hartson SD, Matts RL. Hsp90 regulates p50(cdc27) function during the biogenesis of the active conformation of the heme-regulated eIF2 alpha kinase. J Biol Chem. 2001; 276:206–214. [PubMed: 11036079]

Shao J, Irwin A, Hartson SD, Matts RL. Functional dissection of cdc37: characterization of domain structure and amino acid residues critical for protein kinase binding. Biochemistry. 2003a; 42:12577–12588. [PubMed: 14580204]

Shao J, Prince T, Hartson SD, Matts RL. Phosphorylation of serine 13 is required for the proper function of the Hsp90 co-chaperone, Cdc37. J Biol Chem. 2003b; 278:38117–38120. [PubMed: 12930845]

Siligardi G, Hu B, Panaretou B, Piper PW, Pearl LH, Prodromou C. Co-chaperone regulation of conformational switching in the Hsp90 ATPase cycle. J Biol Chem. 2004; 279:51989–51998. [PubMed: 15466438]

Siligardi G, Panaretou B, Meyer P, Singh S, Woolfson DN, Piper PW, Pearl LH, Prodromou C. Regulation of Hsp90 ATPase activity by the co-chaperone Cdc37p/p50^{cdc37}. J Biol Chem. 2002; 277:20151–20159. [PubMed: 11916974]

Silverstein AM, Grammatikakis N, Cochran BH, Chinkers M, Pratt WB. P50(cdc37) binds directly to the catalytic domain of Raf as well as to a site on hsp90 that is topologically adjacent to the tetratricopeptide repeat binding site. J Biol Chem. 1998; 273:20090–20095. [PubMed: 9685350]

Sobott F, Hernandez H, McCammon MG, Tito MA, Robinson CV. A tandem mass spectrometer for improved transmission and analysis of large macromolecular assemblies. Anal Chem. 2002; 74:1402–1407. [PubMed: 11922310]

Sobott F, Robinson CV. Protein complexes gain momentum. Curr Opin Struct Biol. 2002; 12:729–734. [PubMed: 12504676]

Stancato LF, Chow Y-H, Hutchinson KA, Perdew GH, Jove R, Pratt WB. Raf exists in a native heterocomplex with Hsp90 and p50 that can be reconstituted in a cell-free system. J Biol Chem. 1993; 268:21711–21716. [PubMed: 8408024]

Stebbins CE, Russo AA, Schneider C, Rosen N, Hartl FU, Pavletich NP. Crystal structure of an Hsp90-geldanamycin complex: Targetting of a protein chaperone by an antitumor agent. Cell. 1997; 89:239–250. [PubMed: 9108479]

Stepanova L, Finegold M, DeMayo F, Schmidt EV, Harper JW. The oncoprotein kinase chaperone CDC37 functions as an oncogene in mice and collaborates with both c-myc and cyclin D1 in transformation of multiple tissues. Mol Cell Biol. 2000a; 20:4462–4473. [PubMed: 10825210]

Stepanova L, Leng XH, Parker SB, Harper JW. Mammalian p50(Cdc37) is a protein kinase-targeting subunit of Hsp90 that binds and stabilizes Cdk4. Genes Dev. 1996; 10:1491–1502. [PubMed: 8666233]

Stepanova L, Yang G, DeMayo F, Wheeler TM, Finegold M, Thompson TC, Harper JW. Induction of human Cdc37 in prostate cancer correlates with the ability of targeted Cdc37 expression to promote prostatic hyperplasia. Oncogene. 2000b; 19:2186–2193. [PubMed: 10822368]

Terasawa K, Minami Y. A client-binding site of Cdc37. Febs J. 2005; 272:4684–4690. [PubMed: 16156789]

van Heel M, Harauz G, Orlova EV, Schmidt R, Schatz M. A new generation of the IMAGIC image processing system. J Struct Biol. 1996; 116:17–24. [PubMed: 8742718]

Wan PT, Garnett MJ, Roe SM, Lee S, Niculescu-Duvaz D, Good VM, Jones CM, Marshall CJ, Springer CJ, Barford D, Marais R. Mechanism of activation of the RAF-ERK signaling pathway by oncogenic mutations of B-RAF. Cell. 2004; 116:855–867. [PubMed: 15035987]

Workman P. Combinatorial attack on multistep oncogenesis by inhibiting the Hsp90 molecular chaperone. Cancer Lett. 2004; 206:149–157. [PubMed: 15013520]

Wriggers W, Milligan RA, McCammon JA. Situs: A Package for Docking Crystal Structures into Low-Resolution Maps from Electron Microscopy. J Struct Biol. 1999; 125:185–195. [PubMed: 10222274]

Xu W, Mimnaugh E, Rosser MF, Nicchitta C, Marcu M, Yarden Y, Neckers L. Sensitivity of mature Erbb2 to geldanamycin is conferred by its kinase domain and is mediated by the chaperone protein Hsp90. J Biol Chem. 2001; 276:3702–3708. [PubMed: 11071886]

Xu W, Yuan X, Xiang Z, Mimnaugh E, Marcu M, Neckers L. Surface charge and hydrophobicity determine ErbB2 binding to the Hsp90 chaperone complex. Nat Struct Mol Biol. 2005; 12:120–126. [PubMed: 15643424]

Xu Y, Lindquist S. Heat-Shock Protein Hsp90 Governs the Activity of Pp60(V-Src) Kinase. Proc Natl Acad Sci U S A. 1993; 90:7074–7078. [PubMed: 7688470]

Xu Y, Singer MA, Lindquist S. Maturation of the tyrosine kinase c-Src as a kinase and as a substrate depends on the molecular chaperone Hsp90. Proc Natl Acad Sci USA. 1999; 96:109–114. [PubMed: 9874780]

Zhang W, Hirshberg M, McLaughlin SH, Lazar GA, Grossmann JG, Nielsen PR, Sobott F, Robinson CV, Jackson SE, Laue ED. Biochemical and structural studies of the interaction of Cdc37 with Hsp90. J Mol Biol. 2004; 340:891–907. [PubMed: 15223329]

Zhao Q, Boschelli F, Caplan AJ, Arndt KT. Identification of a conserved sequence motif that promotes Cdc37 and cyclin D1 binding to Cdk4. J Biol Chem. 2004; 279:12560–12564. [PubMed: 14701845]

Europe PMC Funders Author Manuscripts

Europe PMC Funders Author Manuscripts

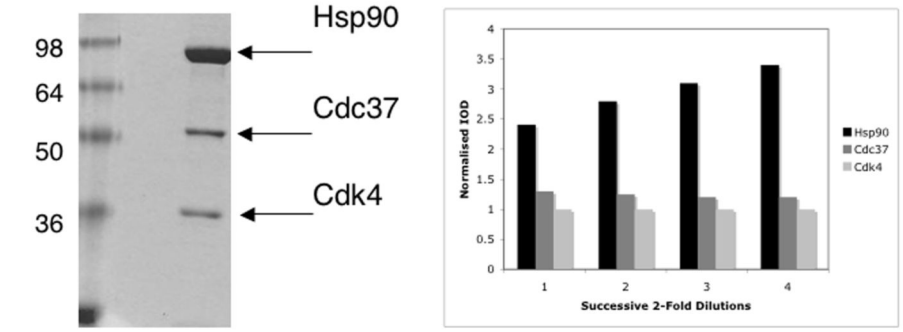

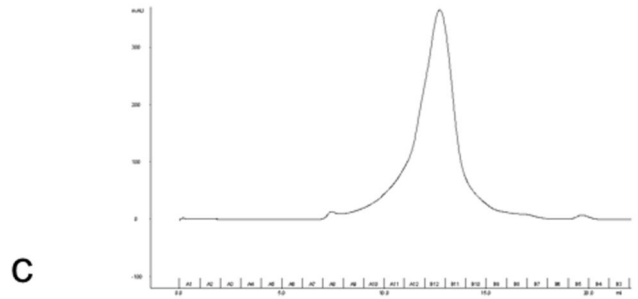

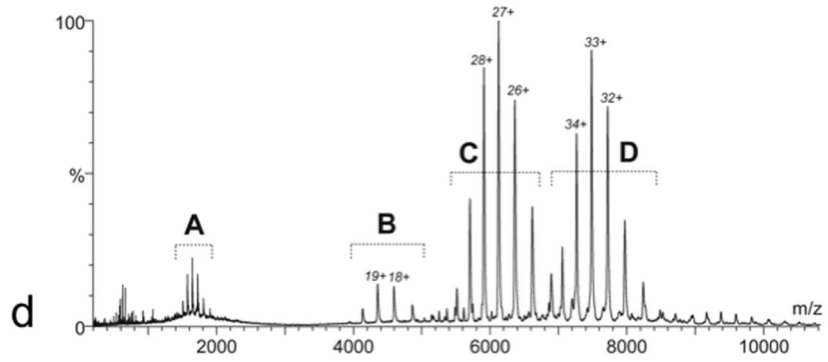

e

Peak series	Measured mass	Species
A	36 173 ±12 Da	Cdk4
B	82 721 ±14 Da	Hsp90
C	165 488 ±44 Da	$(Hsp90)_2$
D	247 113 ±83 Da	$(Hsp90)_2$-Cdc37-Cdk4

Figure 1. Purification and Composition of the Hsp90-Cdc37-Cdk4 Ternary Complex

a) 10% SDS-PAGE of purified Hsp90-Cdc37-Cdk4 (H-C-K) complex.

b) Integrated Optical Density for components of the H-C-K complex for four successive two-fold dilutions in a Coomassie-stained 10% SDS-PAGE. The IOD was normalized by calculated molecular weight of each component and further normalized against the smallest component, Cdk4. The ratio of Cdc37 to Cdk4 remains 1:1 over successive dilutions, in agreement with results from mass spectrometry (see Figure 1d). The Coomassie-binding of Hsp90 is non-linear, possibly as a consequence of the protein's very acidic nature.

c) The final purification step is analytical gel filtration and the chromatogram shows that the proteins run as a single species.

d & e) The Nano-ESI TOF MS spectrum of the complex shows the highest molecular weight species observed in the gas phase is a complex comprising a dimer of Hsp90, a monomer of Cdc37 and a monomer of Cdk4. Masses calculated from the sequences are: Hsp90, 82573 Da; Cdc37, 44468 Da; Cdk4, 35712 Da.

Europe PMC Funders Author Manuscripts

Europe PMC Funders Author Manuscripts

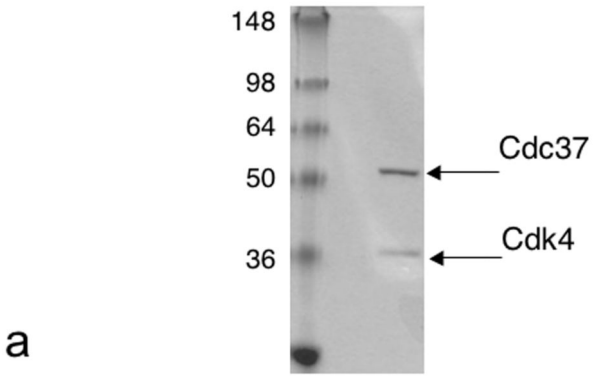

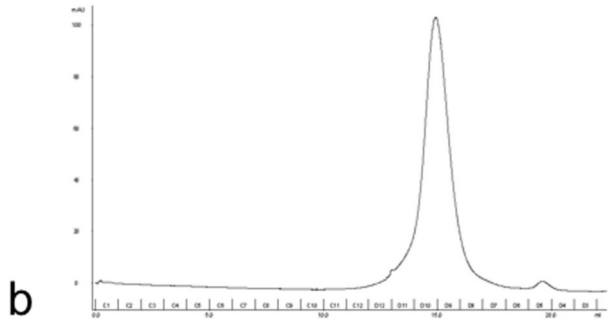

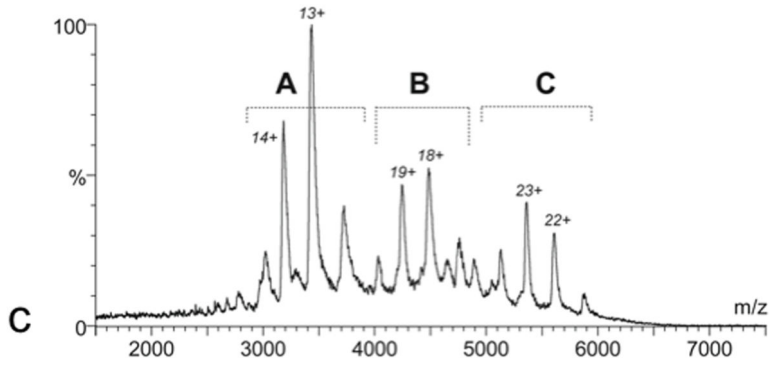

d

Peak series	Measured mass	Species
A	44 574 ±53 Da	Cdc37
B	80 679 ±43 Da	Cdc37 - Cdk4
C	123 384 ±63 Da	$(Cdc37)_2$ - Cdk4

Figure 2. Purification and Composition of the Cdc37-Cdk4 Binary Complex

a) 10% SDS-PAGE of purified Cdc37-Cdk4 (C-K) complex.

b) The final purification step is analytical gel filtration and the chromatogram shows that the proteins run as a single species.

c & d) The Nano-ESI TOF MS spectrum of the complex shows the highest molecular weight species observed in the gas phase is a complex comprising a dimer of Cdc37 and a monomer of Cdk4. Masses calculated from the sequences are: Cdc37, 44468 Da; Cdk4, 35712 Da.

Europe PMC Funders Author Manuscripts

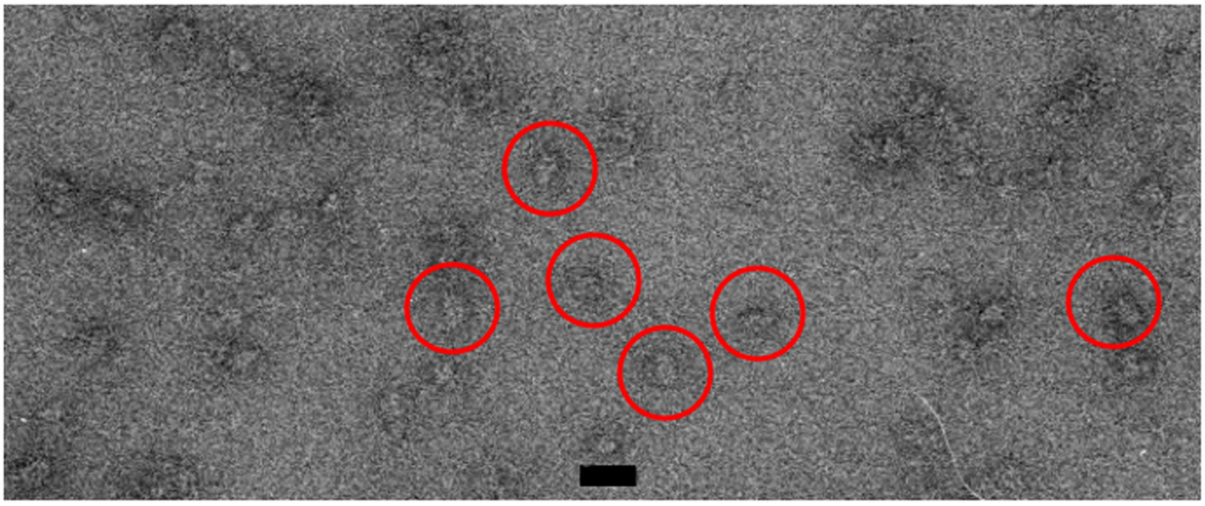

a

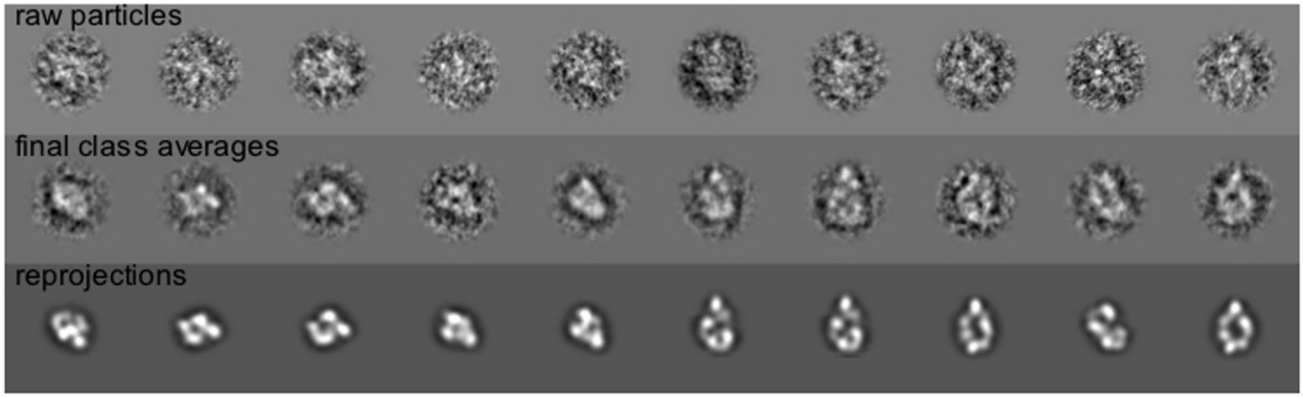

b

Figure 3. Negative-stain Electron Microscopy of Hsp90-Cdc37-Cdk4 Complex

a) A typical micrograph of 2% uranyl acetate-stained H-C-K showing views of the complex. Only particles that were well separated from the others and well stained were picked for analysis. Examples are highlighted in red.

b) Reprojections from the model show features that are recognizable in typical raw particles. Some masked, centred raw particles retrospectively aligned to class averages generated by classification after the final alignment by projection matching. The corresponding reprojections of the model are shown below the class averages.

Europe PMC Funders Author Manuscripts

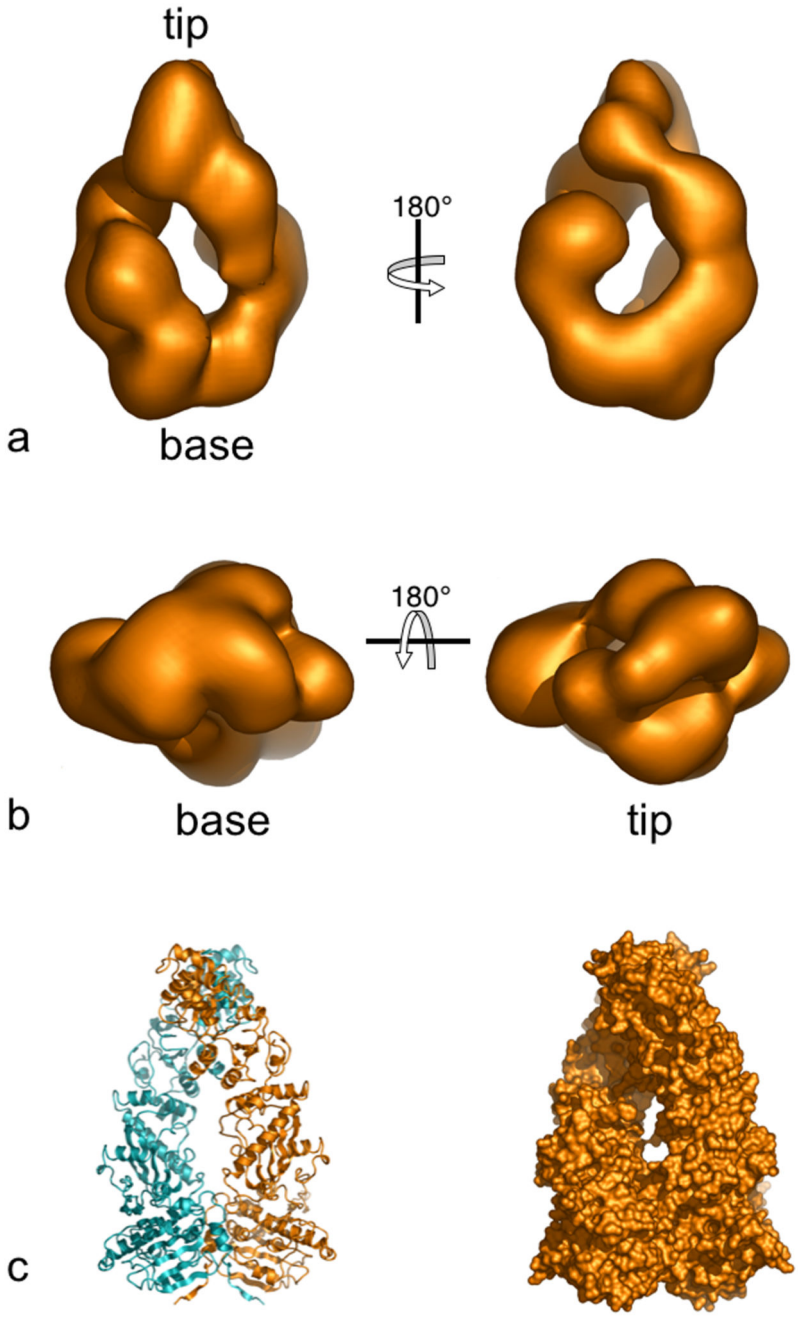

Figure 4. Three-dimensional Reconstruction of Hsp90-Cdc37-Cdk4 Complex

Three-dimensional reconstruction of the H-C-K complex from negative stain electron microscopy.

a) Side views (related by 180º rotation around the vertical) - the oval channel running through the centre of the complex is immediately apparent, as are the two twisting columns of density connecting the base to the tip.

b) End views showing the tip (right) and base (left).

c) Secondary-structure cartoon (left) and molecular surface (right) of the Hsp90 dimer crystal structure (Ali et al., 2006).
Models were generated using MacPyMOL (www.pymol.org).

Europe PMC Funders Author Manuscripts

Europe PMC Funders Author Manuscripts

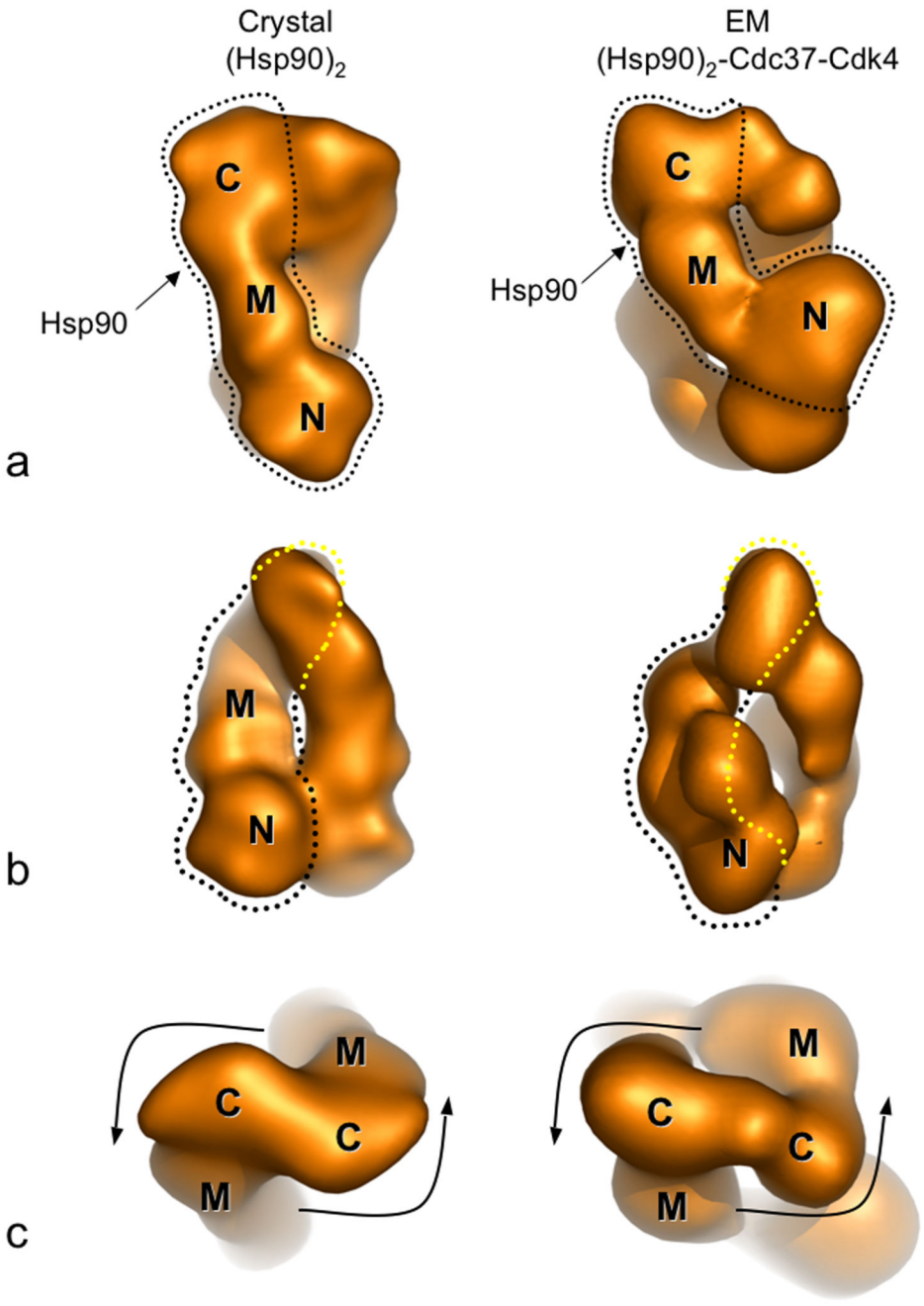

Figure 5. Architecture of the Hsp90-Cdc37-Cdk4 Complex

a & b) Different views of the EM reconstruction, rotated around the vertical axis and corresponding views of the crystal structure, filtered to 20 Å. Equivalent monomers in the crystal structure and the EM reconstruction are outlined in black for each view. By comparison of the two, domains of Hsp90 can be identified. Where one domain is hidden behind another the outline is coloured yellow. There are some interdomain movements on complexation with Cdc37 and Cdk4.

c) The absolute hand of the EM reconstruction can be assigned by matching the twist of the two structures. The C-terminal domain is easily recognised, therefore the polarity of Hsp90 within the model can be determined.

Europe PMC Funders Author Manuscripts

Europe PMC Funders Author Manuscripts

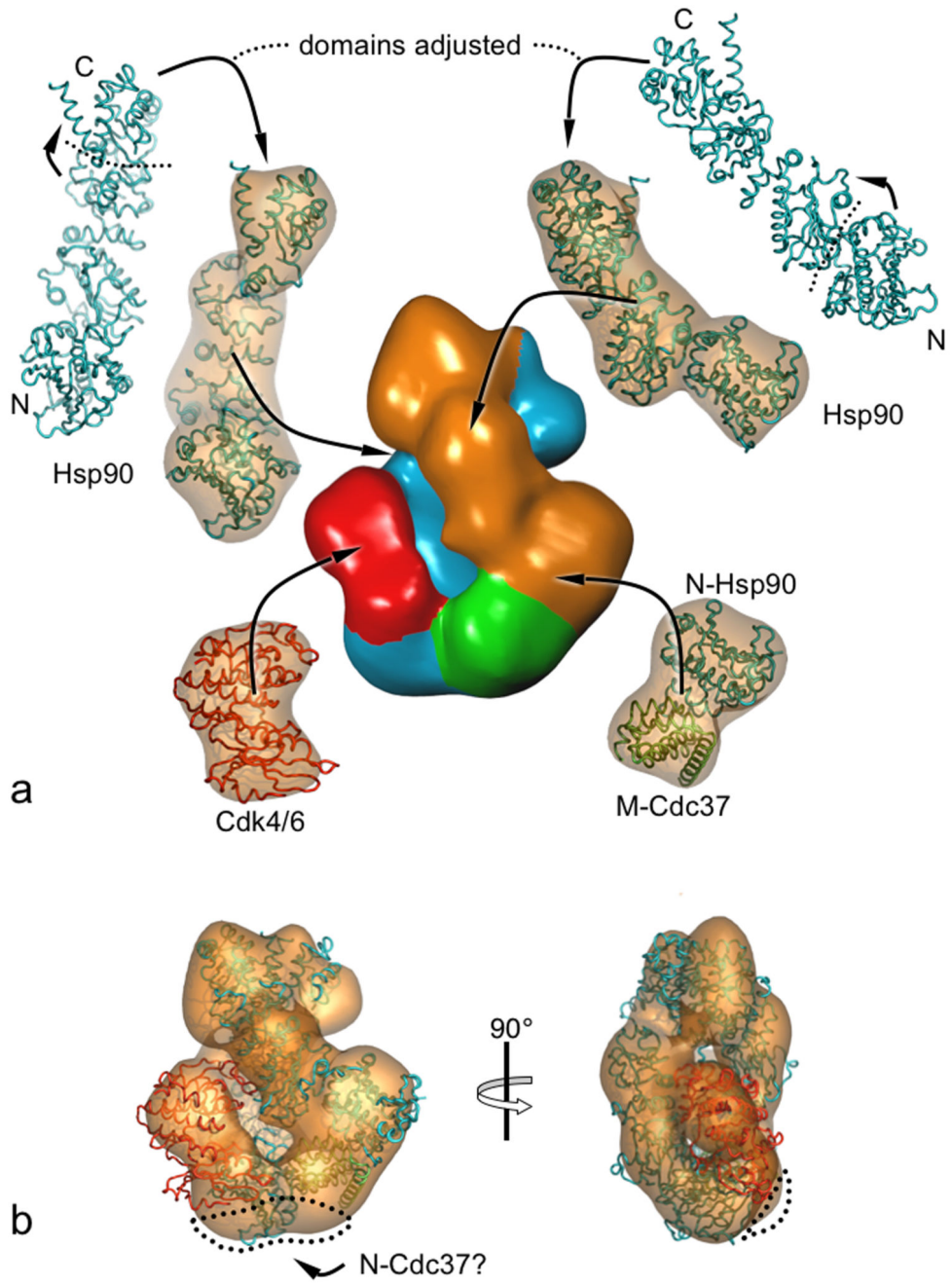

Figure 6. Modelling Cdc37 and Cdk4

a) The relative orientation of domains of the crystal structure of Hsp90 are adjusted by small rotations in the hinge regions and fitted into the EM reconstruction. The location of M-Cdc37 is determined by a least squares fit of the N-terminal domain of the open monomer with N-Hsp90 from the crystal structure of the complex with Cdc37. Cdk6 is used as a model for Cdk4. The larger C-terminal lobe of the kinase fills the larger lobe of the reconstruction and consequently is intimately associated with the middle-domain of one Hsp90 monomer. The N-terminal lobe is smaller and fills the remaining density, associating

with either the N-terminal domain of Hsp90 or Cdc37, or both. Atomic models are shown superimposed on their molecular volumes filtered to 20Å resolution. The EM reconstruction is coloured according to protein chain: Hsp90 open monomer, orange; Hsp90 closed monomer, blue; Cdc37, green; Cdk4, red.

b) Orthogonal views of the pseudo-atomic model of the $(Hsp90)_2$-Cdc37-Cdk4 complex docked into the EM reconstruction. Some unassigned density in the vicinity of the Hsp90 N-termini (dotted outline) could accommodate the N-terminal domain of Cdc37, whose structure is not known, but is predicted to contain a segment of coiled-coil, and could bridge to the N-terminal domain of the closed Hsp90 monomer and/or the bound kinase.

Europe PMC Funders Author Manuscripts

Europe PMC Funders Author Manuscripts

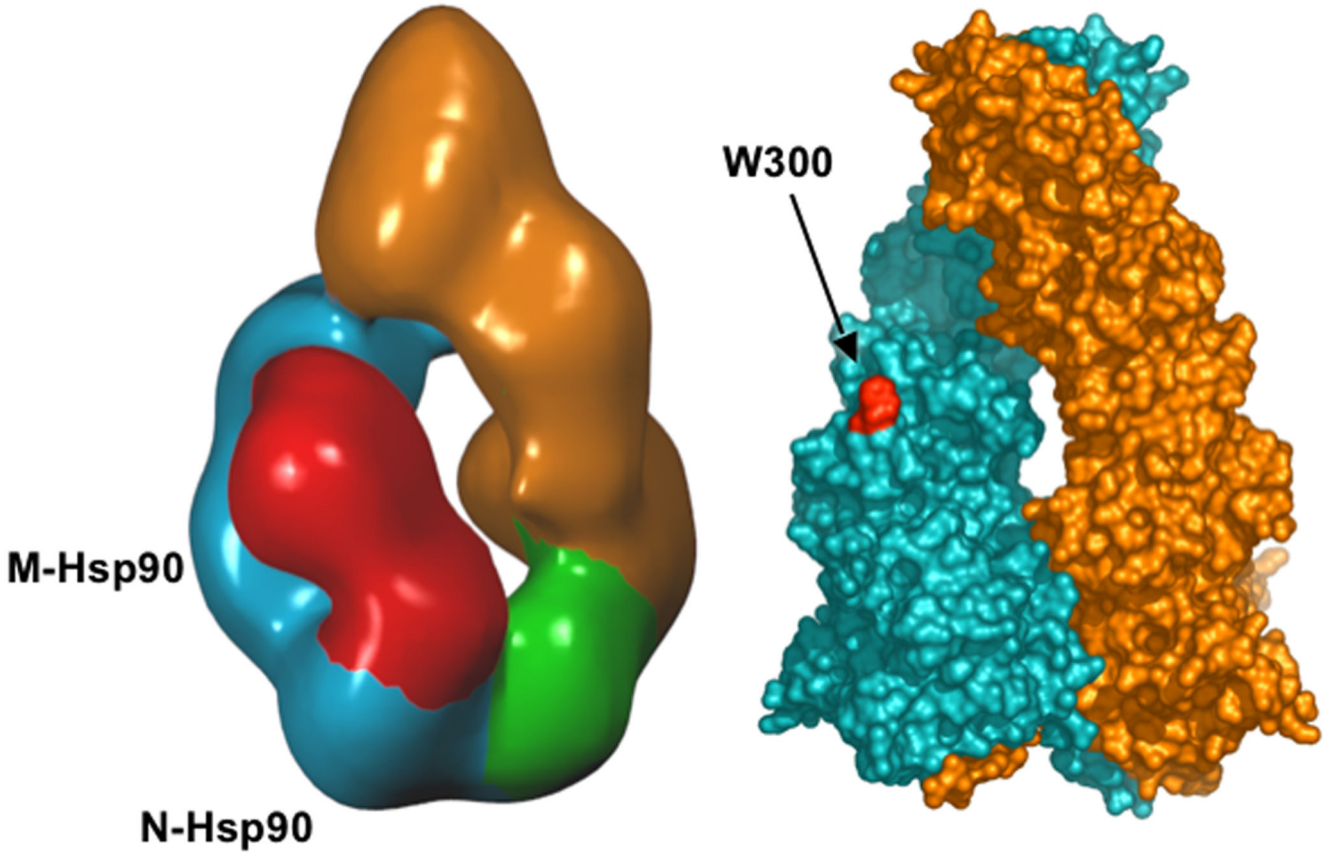

Figure 7. Client Protein Interactions

Comparison of the ~19Å single-particle EM reconstruction (left) of an $(Hsp90)_2$-Cdc37-Cdk4 complex with the ATP-bound Hsp90 crystal structure (right). The bilobal kinase client (red) appears to interact with the N-domain of one Hsp90 protomer and a region on the middle segment close to Trp300 (red on left), which is implicated in client protein binding. Changes in relative position of these Hsp90 domains coupled to the ATPase cycle would be transmitted to the bound client protein.